JOURNAL OF MATERIALS SCIENCE 26 (1991) 1459–1466

Measurements of the craze–bulk interfacial active zone

P. MILLER, E. J. KRAMER
Department of Materials Science and Engineering and the Materials Science Center, Cornell University, Ithaca, New York 14853, USA

The width of the active zone, a region of strain softened material at the craze–bulk interface, was measured as a function of temperature in polystyrene (PS) using a gold decoration technique. Thin trilayer films of PS (total thickness 0.6 μm) with a central layer of buried gold "islands" were made. The films were strained at a controlled rate and various temperatures. When the films crazed, the gold particles act as markers which reveal the deformation of the PS. The strain in the PS could be seen in transmission electron microscopy (TEM) as a change in areal density of the gold particles. The width of the active zone was determined by measuring the distance between the edge of the change in areal density of the gold particles and the craze–bulk interface. It was found that the width of the active zone was a function of the distance behind the craze tip at room temperature. The width of the active zone was ~10 nm at the craze tip and increased linearly to a value of ~25 nm at a distance 250 to 300 μm from the craze tip. The active zone width was independent of the distance from the craze tip for distances greater than 300 μm. The active zone width at the craze tip is in good agreement with previously reported results. The higher strain rates at the craze tip are believed to be responsible for the change in the width of the active zone as a function of distance behind the craze tip. The active zone width increased linearly with increasing temperature from 25 nm at room temperature to 60 nm at 93 °C. The increase in the active zone width can be accounted for by the decrease in strain softening of PS at higher temperatures.

1. Introduction

The fracture of glassy polymers has been linked to the formation and breakdown of crazes. A craze is a localized region of plastic deformation which is characterized by fibrils which span the craze–bulk interface. The fibrils allow the craze to support a load, but subsequent rupture of the fibrils can create sites for crack nucleation. A crack of critical size may form by slow breakdown of neighbouring fibrils and propagate along the length of the craze causing macroscopic failure [1–4].

Once formed, crazes widen by drawing new material into the fibrils from the active zone [4]. The active zone is a thin region of strain softened polymer at the craze–bulk interface. Entangled polymer strands in the active zone bridging two fibrils must either disentangle or undergo scission in order to create new fibril surfaces. It has been found that for polystyrene (PS) chain scission is the dominant mechanism for loss of entangled strands during crazing at room temperature, with nearly one half of the strands broken during fibrillation [5]. At higher temperature ($T > 50\,^{\circ}C$), the disentanglement of polymer chains becomes more important [6].

The width of the active zone, h, is an important parameter in describing craze kinetics. It can be shown that the crazing stress, S_C, is a function of h [4]. The relative values of S_C and S_{DZ}, the stress to form a shear deformation zone, determine whether crazes or DZs are formed [7–9]. In the past it has been assumed that h was independent of the crazing temperature [8]. In order to model accurately the transition from crazes to DZs at high temperatures, a knowledge of h as function of temperature is needed.

While observation of the active zone of crazes in undecorated films is difficult in transmission electron microscopy (TEM), it is possible to reveal the active zone by using gold particles as markers. Gold decoration is accomplished by the vacuum deposition of gold on to PS to create small, discrete gold "islands" on the polymer surface. These "islands" are dragged along by the polymer as the material deforms and examination of the gold markers in TEM provides a method of measuring h.

This paper demonstrates the usefulness of the gold decoration technique for measuring h. The width of the active zone is measured as a function of temperature and compared to previous results. The active zone width as a function of temperature, $h(T)$ is calculated from previous results of the crazing–DZ

0022–2461/91 $03.00 + .12

transition envelope [8]. It is shown that the calculated value of $h(T)$ is in reasonable agreement with the experimentally determined value of $h(T)$.

2. Experimental procedure

Nearly monodisperse PS with a molecular weight $M_w = 390000$ which had a polydispersity index $M_w/M_n < 1.2$ was purchased from the Pressure Chemical Company. Thin films of the polymer were cast on glass slides by drawing at a constant rate from a methylene chloride solution. The films were determined to be approximately 0.3 μm thick as measured by a Zeiss interference microscope. After the solvent had evaporated, one half of the samples were placed in a vacuum evaporator and a thin layer of gold was deposited on the top surface of the PS. The average areal density of the gold layer was determined to be 8×10^{15} atom cm^{-2} by Rutherford backscattering spectrometry (RBS).

The as-cast films were floated off the slides on to the surface of a water bath and picked up on the gold-coated glass films to create a PS–gold–PS "sandwich" with a total thickness of 0.6 μm. Subsequent examination in TEM determined that this step did not significantly alter the morphology of the gold particles. After the water had completely evaporated, the samples were exposed to methylene chloride vapour for approximately one minute to bond the two PS films together to facilitate handling.

The trilayer film was then cut into small rectangular sections and floated off the slide on to the surface of a water bath. The sections were picked up from the bath and deposited on to the surface of freshly cleaved salt crystals. The films on the salt crystal substrate were placed in a vacuum oven (pressure $< 10^{-3}$ Torr) at 178 °C for 66 min. Previous experiments by Green *et al.* have shown that annealing under these conditions causes the two polymer films to interdiffuse and bond permanently together [10]. Fig. 1 is a TEM micrograph showing the initial distribution of gold particles in a trilayer film.

After the anneal, the films were floated on the surface of a water bath by dissolving the salt crystals and picked up on annealed copper grids, the grid bars of which had been previously coated with PS. A brief exposure to methylene chloride vapour bonded the films to the copper grids. The samples were then placed back in the vacuum oven at 90 °C for 11 h to remove residual solvent and to physically age the films*. Starter cracks ~ 80 μm long were burnt into suitable film squares (ones with few dust particles or large defects) with a focused electron beam from a JEOL 733 microprobe [11].

The grids were mounted in a strain frame in an oven. The strain frame was driven by a constant speed motor at a strain rate of 4.2×10^{-6} sec^{-1} at various temperatures. The total plastic strain was approximately 0.015 to 0.02. The samples were examined with

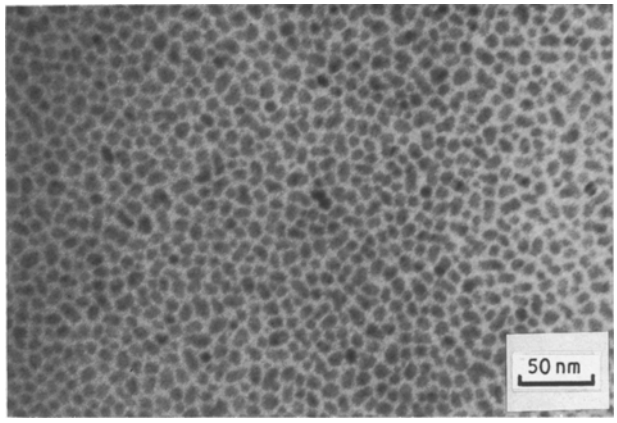

Figure 1 A TEM micrograph of a trilayer gold film after a 1 h anneal at 178 °C. The gold islands are ~ 80 nm in diameter.

an optical microscope and a film square that contained an isolated craze growing from the starter crack was selected. This film square was carefully cut from the sample and mounted in a JEOL 200CX TEM sample holder such that the length of the craze was parallel with the sample holder tilt axis. The specimen was tilted ± 10° in 2° steps and micrographs were taken of the gold particles at craze–bulk interface at each step.

3. Results

Fig. 2a is a schematic of a trilayer sample. For the purpose of simplicity, the craze is depicted as containing regular array of fibrils and the same areal density of the gold particles is depicted in the fibrillated region and in the active zone. Initially, the gold particle coverage is uniform throughout the sample. After a craze is formed and begins to widen, polymer chains in the active zone and the fibrils are drawn to higher extensions than in undeformed material. Since the gold particles are drawn into the fibrils with the polymer, the areal density of gold particles is decreased in the plastically deformed regions of the active zone and the fibrils as compared to the undeformed bulk film.

The width of the active zone can be measured by determining the distance between the edge of the region of decreased gold areal density and the craze–bulk interface. If the sample is not normal to the z axis (the direction of electron beam) then the craze–bulk interface will appear broadened in TEM making an accurate measure of the active zone width difficult to obtain as illustrated in Fig. 2b. Note that the width of the active zone and the thickness of the sample are not drawn to scale in this schematic.

By tilting the sample along an axis parallel to the length of the craze, it is possible accurately to determine when the craze–bulk interface is parallel to the z axis. Fig. 3a to c are TEM micrographs of the

* Polymer ageing is accelerated at temperatures close to the glass transition temperature and can effect the mechanical properties of the polymer. By ageing the samples at a high temperature for times much greater than the testing time, it was possible to assure that all the samples had a similar ageing history despite differences in the testing temperature.

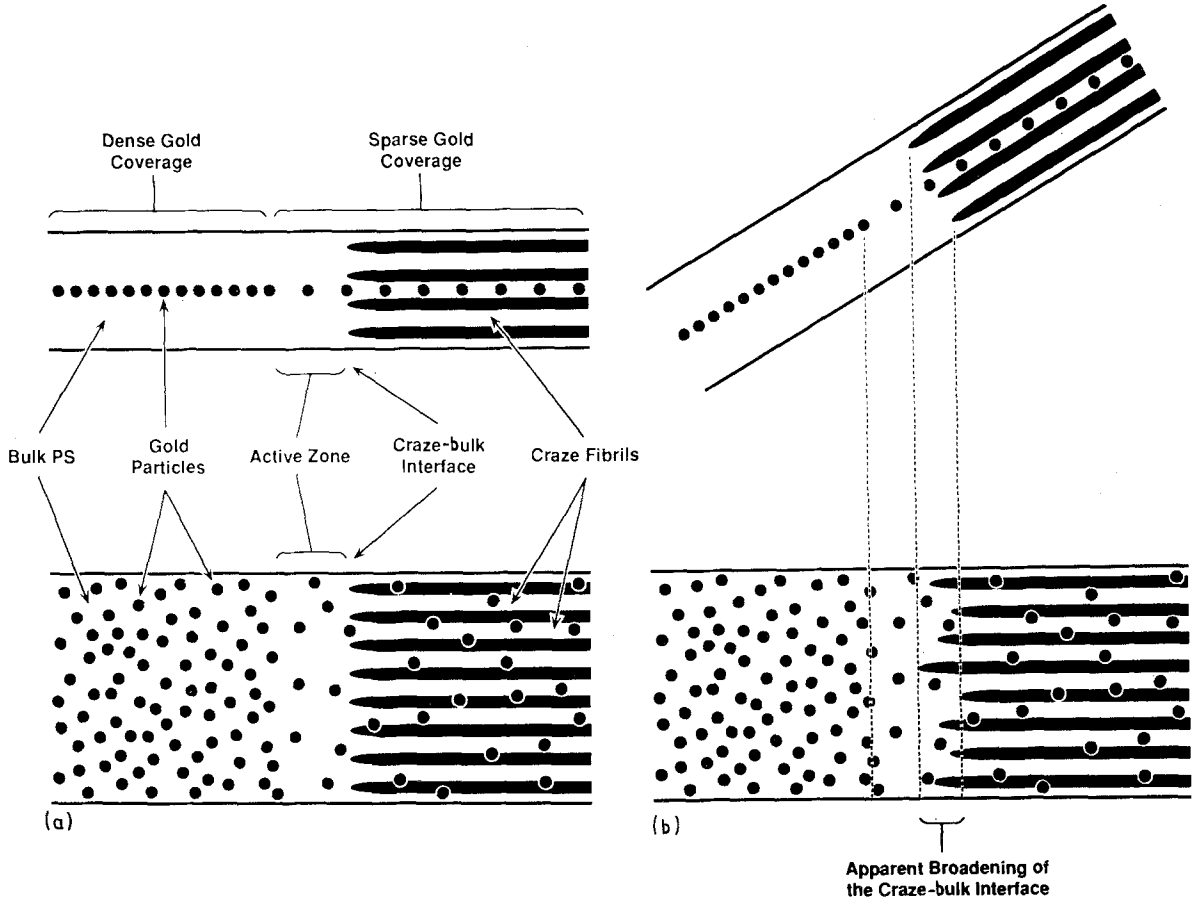

Figure 2 A schematic of the craze–bulk interface in a trilayer sample (a) normal to the electron beam and (b) tilted with respect to the electron beam. Note that the width of the active zone and the sample width are not to scale. The side view is shown at the top and the top view at the bottom.

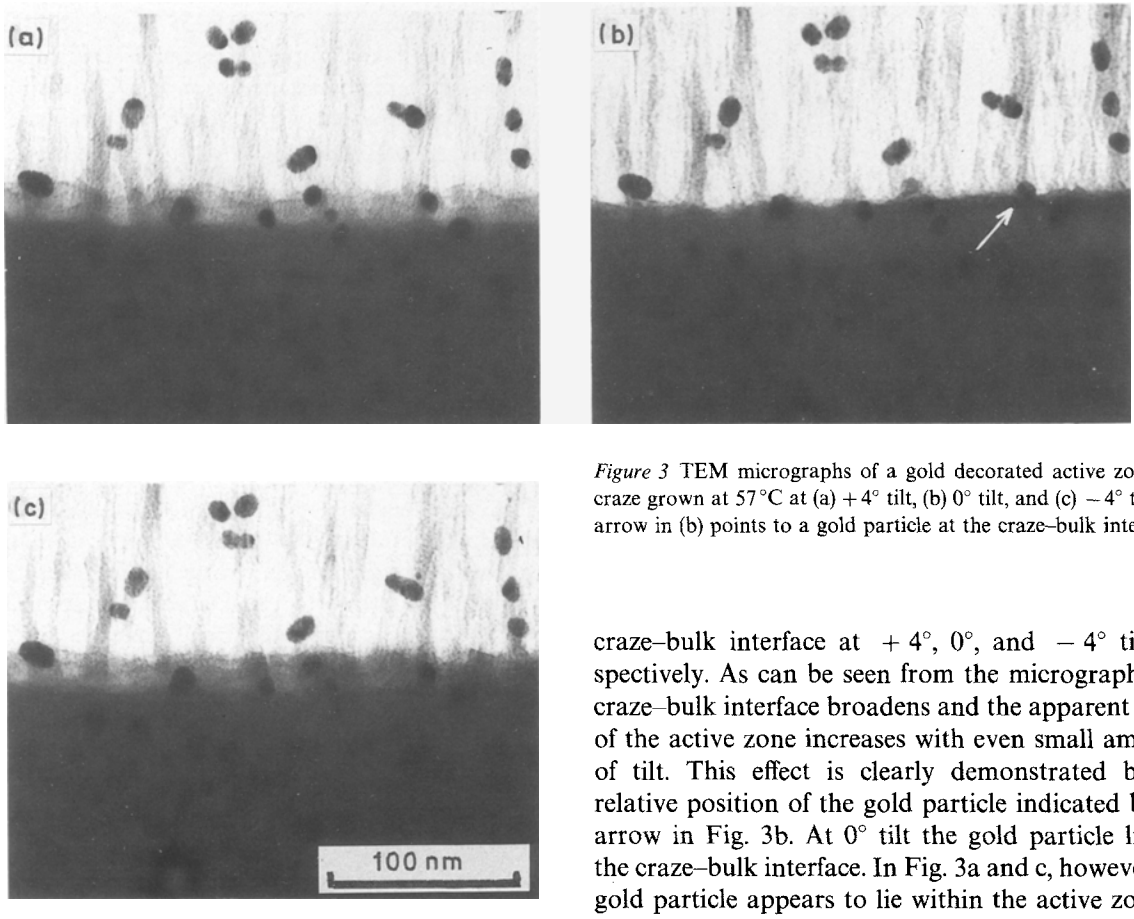

Figure 3 TEM micrographs of a gold decorated active zone of a craze grown at 57 °C at (a) +4° tilt, (b) 0° tilt, and (c) −4° tilt. The arrow in (b) points to a gold particle at the craze–bulk interface.

craze–bulk interface at + 4°, 0°, and − 4° tilt, respectively. As can be seen from the micrographs, the craze–bulk interface broadens and the apparent width of the active zone increases with even small amounts of tilt. This effect is clearly demonstrated by the relative position of the gold particle indicated by the arrow in Fig. 3b. At 0° tilt the gold particle lies on the craze–bulk interface. In Fig. 3a and c, however, the gold particle appears to lie within the active zone.

The apparent change in width of the active zone with various angles of tilt is due to the fact that a TEM micrograph is a two-dimensional projected image of a three-dimensional structure. This problem is accentuated because the width of the active zone is much smaller than the thickness of the sample. However, by examining a series of micrographs taken at various degrees of tilt, it is relatively easy to determine when the craze–bulk interface is parallel to the z axis: the craze–bulk interface becomes well defined when the film is properly aligned.

The micrographs in Fig. 4 may be used as a stereographic pair. The stereographic image clearly shows that the gold particles lie in the middle of the film. In addition, the gold particle indicated in Fig. 3b is seen to lie on the craze–bulk interface.

It was found that the width of the active zone was not uniform along the length of the craze. The width of the active zone is plotted as a function of the distance from the starter crack in Fig. 5. This graph shows that h is smallest at the tip of the craze. (This figure is only meant to show the trend of active zone width as a function of the craze length. Absolute values of h cannot be determined from this plot since this sample was not tilted to align the craze–bulk interface parallel to the electron beam.) Measurements of h in different samples must be taken at a constant distance from the craze tip in order to be able to make meaningful comparisons of the data.

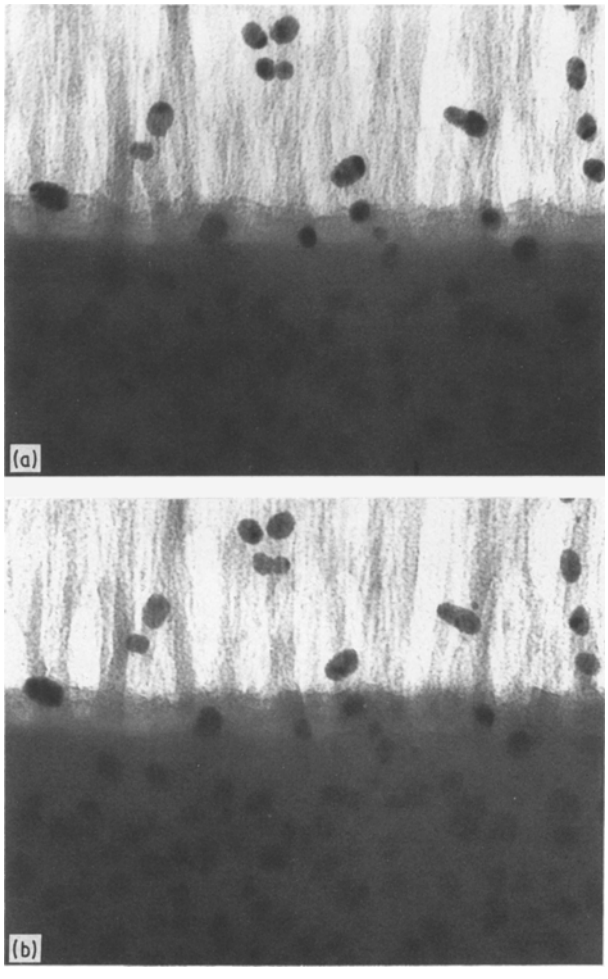

Figure 4 A stereopair of TEM micrographs of a gold decorated active zone of a craze grown at 57 °C.

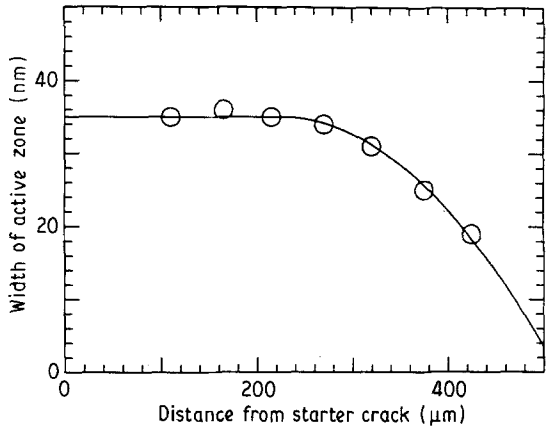

Figure 5 A plot of the width of the active zone against distance along the craze from the starter crack. Note: absolute values of the active width may not be determined from this plot since this sample was not tilted normal to the electron beam.

Since the crazes in our samples typically grew to the edge of the copper grids, this procedure could not be followed. It is possible to get consistent results, however, by measuring h at constant craze width; the width of a craze is proportional to the distance from the craze tip in regions sufficiently far from the tip. The data that follow are all taken at a constant craze width of ~ 3 μm.

Fig. 6a to f are TEM micrographs of the craze–bulk interface at 23, 39, 57, 68, 84 and 93 °C, respectively. The micrographs displayed here are of samples which were tilted such that the craze–bulk interface was parallel to the electron beam to provide accurate measures of the active zone width by the procedure outlined above. Fig. 7 is a plot of the width of the active zone taken from these samples and others as a function of crazing temperature. It is clear from these data that the width of the active zone increases with increasing temperature contrary to previous assumptions [8].

4. Discussion

4.1. Crazing temperature and strain rate effects

A typical true stress–strain curve for a glassy thermoplastic is shown in Fig. 8 based on work by Bowden and Raha [12]. In region A, the polymer deforms elastically. Beyond the yield point, the polymer strain softens (region B) and then strain hardens (region C). The exact mechanism for strain softening of the polymer in region B is not well understood, although it is generally accepted that a change in the structure of the polymer glass due to shear strain is responsible for strain softening. Several models have been proposed to describe the yielding behaviour of glassy polymers with various degrees of success [13–16].

Phenomenologically, the strain softening of a polymer in compression is found to depend on several parameters. It has been determined that increasing the temperature of the test decreases the yield stress and the amount of strain softening of a polymer [12]. The thermal history of a specimen also affects its strain

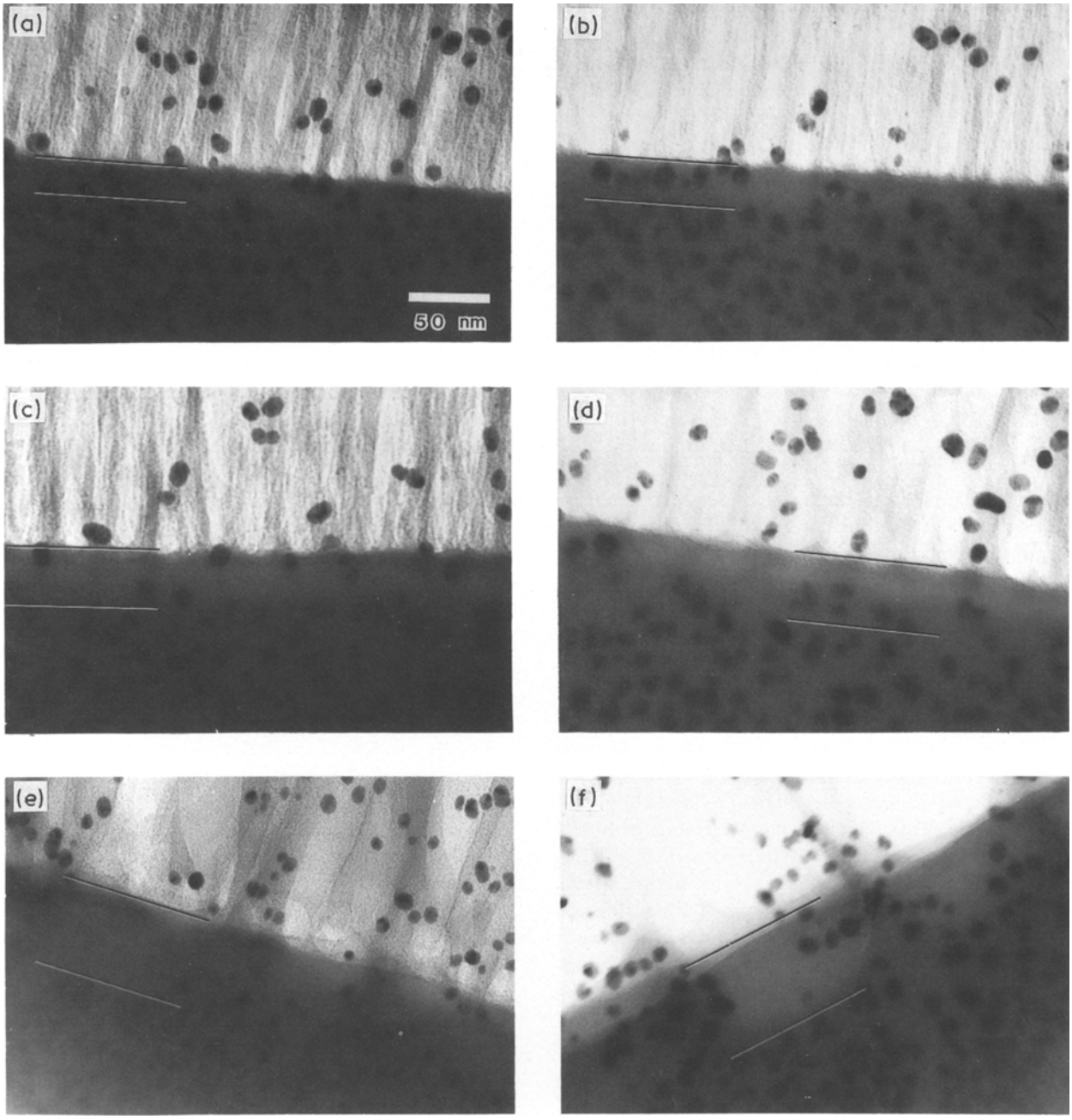

Figure 6 TEM micrographs of gold decorated active zones of crazes grown at (a) 23 °C, (b) 39 °C, (c) 57 °C, (d) 68 °C, (e) 84 °C, and (f) 93 °C.

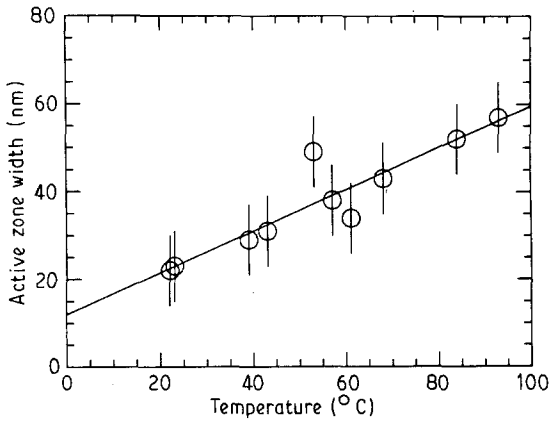

Figure 7 A plot of the width of the active zone as a function of the crazing temperature.

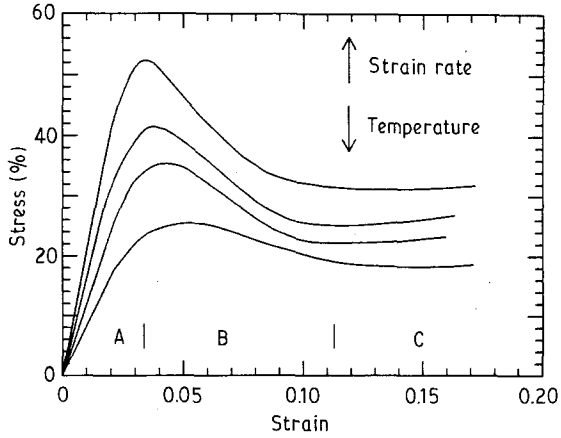

Figure 8 A schematic plot of the true stress against true strain for PS in compression after Bowden and Raha showing elastic deformation (A), strain softening (B), and strain hardening (C). The arrows indicate increasing temperature and increasing strain rate.

softening; it has been found that samples of PS which were cooled slowly after an anneal above T_g exhibit more strain softening than samples which were cooled quickly [12]. An increase in strain rate also increases the amount of strain softening in glassy polymers [12, 16].

Strain localization is a natural consequence of strain softening. Qualitatively, an inhomogeneity such as a dust particle or void will cause local rise in stress. As the stress on the sample is increased, the material near the inhomogeneity will yield first. This material will strain soften and its yield stress will be less than the rest of the sample, thus, further deformation will be accommodated by the continued yielding of the strain softened material and the strain will localize.

Since strain localization inevitably accompanies strain softening, it is found that the same conditions that increase strain softening also enhance the localization of strain. Shear deformation zones in thin films of physically aged polycarbonate (PC) strained in tension are more diffuse than DZs grown in as-cast PC [11]. Similarly, the tendency to form localized shear bands in PS in compression tests is decreased if the samples are quenched rapidly from the melt [17]. Decreasing the temperature or increasing the strain rate of the compression tests tends to localize the shear bands in PS [11].

The active zone is a region of inhomogeneous yield that occurs in crazed samples strained in tension. Is it reasonable to compare the plastic deformation that occurs in PS strained in tension to results obtained from samples strained in compression when describing the processes that lead to the formation of the active zone? Although the yielding of PS in tension and compression is analogous, the processes are not identical due to the normal stresses which are dilatational in the former case and compressive in the latter case [18]. The chief difference in the two types of yielding is the tendency for neck formation in tensile samples and, in the case of crazing, the formation of a void structure. However, since the mechanism for strain softening is presumed the same for both types of yielding (i.e. a restructuring of the polymer glass), it is reasonable to expect the strain softening in the active zone of a craze to follow the same trends as the strain softening in shear bands.

The decrease in strain softening as a function of temperature is shown schematically in Fig. 8. Since it has been shown that degree of strain localization is proportional to the amount of strain softening that a polymer undergoes, one expects the strain localization to decrease with increasing temperature, thus, the increase of the width of the active zone at high temperatures is believed to be due to the decreased strain softening in this regime. This assumption is supported by observations of shear bands in PS strained in compression; it was found that there is a transition from shear bands to diffuse shear zones at higher temperatures [11].

Since the degree of strain softening is also found to be dependent on the strain rate, arguments similar to the one outlined above can be used to explain the decrease of h at the craze tip. There are two mechanisms involved in the growth of a craze: craze tip advance and craze widening [4, 19]. The craze tip advances faster than the craze widens; this fact is evident from the long, thin shape of a typical craze. In addition, the rate of widening of the craze is not uniform along the length of the craze, but is somewhat faster just behind the craze tip [20].

Fig. 9 is a plot of the width of a craze as a function of the distance from the starter crack. It can be seen from this graph that width of the craze, τ, increases uniformly over most of the body of the craze. This portion of the graph can be fitted with a straight line. The rate of craze widening, $d\tau/dt$, can be determined from the slope of the tangent to curve in Fig. 9 if the rate of craze tip advance is known. A typical rate of craze tip advance in these experiments was $\sim 0.4\ \mu m\ sec^{-1}$.* Thus, for the body of the craze $(d\tau/dt)_{body} \approx 0.4\ nm\ sec^{-1}$ [20]. At the craze tip, it is found that $(d\tau/dt)_{tip}$ is approximately a factor of three higher than $(d\tau/dt)_{body}$. Qualitatively, since the width of the craze at the tip is less than the projected average (the dashed line in Fig. 9), the portion of the craze just behind the tip must widen at a faster rate to achieve the average value.

Just as increasing the testing temperature reduced the degree of strain softening and decreased the amount of strain localization, faster strain rates will also produce smaller regions of inhomogeneous strain [11], thus the larger strain rates at the craze tip due to the process described above will produce narrow active zones. As the craze widens, the strain rate drops and wider active zones are produced as the strain is delocalized.

When the slope of the craze width against craze length curve becomes constant, the active zone width should be independent of the craze width. From Fig. 9, the craze widening rate becomes constant at distances between 250 to 350 μm from the starter crack. As shown in Fig. 5, the width of the active zone becomes constant at values $\sim 250\ \mu m$ from the starter crack.

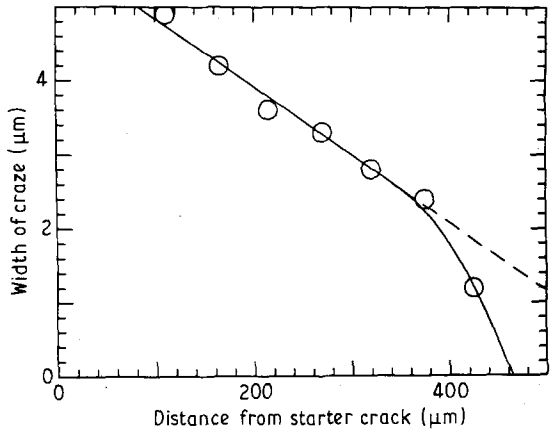

Figure 9 A plot of the craze width against the distance from the starter crack of a craze in PS grown at room temperature.

*Assuming that the craze nucleated at $\varepsilon = 0.007$, the total time of craze growth was ~ 2000 sec at a nominal strain rate of $4.2 \times 10^{-6}\ sec^{-1}$. The total craze length was $\sim 750\ \mu m$ and therefore the rate of craze tip advance was approximately $0.4\ \mu m\ sec^{-1}$.

The width of the active zone has been previously reported in the literature as 5 to 20 nm by Donald and Kramer [19]. These measurements were made on gold-decorated PS films that were strained by hand. Donald and Kramer were examining the Taylor meniscus instability model of craze tip advance and focused their attention on the regions of the craze just behind the craze tip. Data from crazes in our experiments which had not grown to the edge of the copper grid yield a value of ~ 10 nm when extrapolated to the craze tip which is in reasonable agreement with the previous result. Furthermore, it is expected that the active zone widths measured by Donald and Kramer would be narrower than the active zone widths measured in this paper due to the faster strain rates in the Donald and Kramer experiments.

4.2. The effects of the active zone width on craze kinetics

Previous work has shown that by crosslinking PS with electron radiation it is possible to induce a transition from crazing to the formation of shear deformation zones (DZs) for thin films strained in tension [7, 9]. The transition occurs at a critical strand density, ν_t, which is a function of the sample temperature [8]. The crazing stress, S_c, is given by [4]

$$S_c \propto \left(\frac{\sigma_{y(craze)}\Gamma}{h}\right)^{1/2} \quad (1)$$

where $\sigma_{y(craze)}$ is the yield stress of the material in the active zone. The energy required to create new fibril surface, Γ, is given by

$$\Gamma = \gamma + \tfrac{1}{4}Ud\nu \quad (2)$$

where γ is the van der Waals surface energy of intermolecular separation, U the energy needed to break a main chain bond, and d the network mesh size. The mesh size can be written as

$$d = k\left(\frac{\rho N_A}{\nu}\right)^{1/2} \quad (3)$$

where k is a constant of proportionality which can be determined from measurements of the molecular coil size, ρ the density of the polymer, and N_A Avogadro's number. Since d is proportional to $\nu^{-1/2}$, the product $d\nu$ is proportional to $\nu^{1/2}$, thus, Equation 1 can be rewritten as

$$S_c \propto \left(\frac{\sigma_{y(craze)}(\gamma + c\nu^{1/2})}{h}\right)^{1/2} \quad (4)$$

where c is a constant. It is clear from this equation that S_c increases with increasing ν. DZs are formed by the motion of molecular segments smaller than the strand length and thus the stress to form a deformation zone, S_{DZ}, is approximately independent of ν

$$S_{DZ} \propto \sigma_{y(DZ)} \quad (5)$$

The transition from crazing to the formation of DZs occurs at the critical value of ν such that $S_c = S_{DZ}$.

Fig. 10a shows the transition from crazes to DZs at various temperatures that was observed by Berger and Kramer [8]. Previously, it has been assumed that the

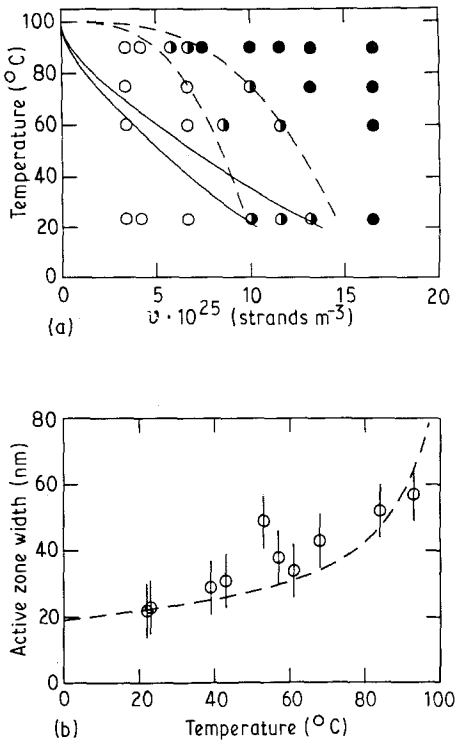

Figure 10 (a) A deformation map for PS as a function of strand density and temperature from [8]. The open circles represent samples that crazed, the full circles represent samples that formed shear deformation zones, and the half-full circles represent samples that underwent both types of deformation. The dashed lines show the experimentally determined ν_t envelope and the solid lines show the transition envelope as determined from Equation 6. (b) A plot of the width of the active zone against crazing temperature. The dashed line corresponds to the temperature dependent function $h(T)$ in Equation 6 to produce the experimentally determined ν_t curves in (a).

width of the active zone of a craze is independent of the crazing temperature. The shift in ν_t to lower values of ν has been explained by the relative sensitivity of S_c and S_{DZ} to changes in the yield stress as a function of temperature. At some temperature T_1, $S_c = S_{DZ}$ at the value $\nu = \nu_{t(T_1)}$. Equation 1 shows that S_c depends on $\sigma_y^{1/2}$ whereas from Equation 5 it is seen that S_{DZ} is proportional to σ_y. From Fig. 8 it is apparent that σ_y decreases with increasing temperature, thus S_{DZ} decreases faster than S_c with increasing temperature and at $T_2 < T_1$, $S_c > S_{DZ}$ at $\nu = \nu_t(T_1)$. At temperature T_2, S_c will only equal S_{DZ} at a value $\nu = \nu_t(T_2)$, where $\nu_t(T_2) < \nu_t(T_1)$, thus transition from crazing to the formation of DZs is shifted to lower values of ν as the sample temperature is increased.

We now know, however, that the width of the active zone increases with the crazing temperature, and does not remain constant as was previously thought. Since h increases with temperature, it can be seen from Equation 1 that S_c will decrease with increasing temperature more rapidly than $\sigma_y^{1/2}$.

By assuming that $\sigma_{y(craze)} = \sigma_{y(DZ)} = \sigma_y(T)$ it is possible to generate theoretical curves of ν_t as a function of temperature from Equations 1 and 2:

$$\nu_t = A[\sigma_y(T)h(T) - B]^2 \quad (6)$$

where A and B are determined from the condition that $\nu_t = 0$ at $T = T_g$ and from the two experiment-

ally determined room temperature values of ν_t: $\nu_t = 9.9 \times 10^{25}$ strands m^{-3} and $\nu_t = 13.2 \times 10^{25}$ strands m^{-3} [8]. Berger and Kramer used this method to calculate $\nu_t(T)$ using a temperature independent value for h; their results are shown as the solid lines in Fig. 10a. Although their curves predict the correct trend of ν_t as a function of temperature, the calculated $\nu_t(T)$ curves do not match the experimentally determined transition envelope (dashed lines).

From Equation 6 it is obvious that ν_t is strongly dependent on h. It is possible to calculate the temperature dependence of the width of the active zone necessary to produce the experimentally determined curves of ν_t in Fig. 10a. The calculated value of $h(T)$ is shown as the dashed line in Fig. 10b. This curve is in reasonable agreement with the experimental data. It should be noted that the assumption that $\sigma_{y(craze)} = \sigma_{y(DZ)}$ may not be strictly accurate, and thus it may not be possible to determine precisely $h(T)$ from Equation 6. It is evident, however, from this example that it is necessary to know the temperature dependence of h to predict accurately craze kinetics and the craze to shear transition.

5. Conclusions

The conclusions are as follows.

(1) The width of the active zone, the strain softened region at the craze–bulk interface, increases with increasing temperature due to the decrease in strain softening of polystyrene at higher temperatures.

(2) The width of the active zone is a function of distance from the craze tip, increasing from ~ 10 nm at the craze tip to ~ 25 nm at distances far from the tip at room temperature.

(3) A knowledge of h as a function of the crazing temperature allows one to predict the craze to shear transition as a function of temperature and network strand density.

Acknowledgements

The support of this work by the Cornell Materials Science Center which is funded by the National Science Foundation, DMR-MRL is gratefully acknowledged. Philip Miller was supported by a fellowship provided by the Mobil Chemical Company.

References

1. S. RABINOWITZ and P. BEARDMORE, *CRC Rev. Macromol. Sci.* **1** (1972) 1.
2. R. P. KAMBOUR, *J. Polym. Sci. Macromol. Rev.* **7** (1973) 1.
3. A. N. GENT, "The Mechanics of Fracture, AMD", Vol. 19, edited by F. Erdogon (ASME, New York, 1976) p. 55.
4. E. J. KRAMER, "Microscopic and Molecular Fundamentals of Crazing" (*Adv. Polym. Sci.* **52/53**) (Springer, Berlin, 1983) p. 7.
5. C. C. KUO, S. L. PHOENIX and E. J. KRAMER, *J. Mater. Sci. Lett.* **4** (1985) 459.
6. L. L. BERGER and E. J. KRAMER, *Macromolecules* **20** (1987) 1980.
7. C. S. HENKEE and E. J. KRAMER, *J. Polym. Sci., Polym. Phys.* **22** (1984) 721.
8. L. L. BERGER and E. J. KRAMER, *J. Mater. Sci.* **23** (1988) 3536.
9. P. MILLER, PhD Thesis, Cornell University (1987).
10. P. F. GREEN, C. J. PALMSTROM, J. W. MAYER and E. J. KRAMER, *Macromolecules* **18** (1985) 501.
11. A. M. DONALD and E. J. KRAMER, *J. Mater. Sci.* **16** (1981) 2967.
12. P. B. BOWDEN and S. RAHA, *Phil. Mag.* **22** (1970) 463.
13. R. E. ROBERTSON, *J. Chem. Phys.* **44** (1966) 3950.
14. I. M. WARD, *J. Mater. Sci.* **6** (1971) 1397.
15. A. S. ARGON, *Phil. Mag.* **28** (1973) 839.
16. R. N. HAWARD, "The Physics of Glassy Polymers", edited by R. N. Haward (Applied Science, London, 1973) p. 340.
17. T. E. BRADY and G. S. Y. YEH, *J. Appl. Phys.* **42** (1971) 4622.
18. R. N. HAWARD, B. M. MURPHY and E. F. T. WHITE, *J. Polym. Sci.* **A9** (1971) 801.
19. A. M. DONALD and E. J. KRAMER, *Phil. Mag.* **A43** (1981) 857.
20. A. M. DONALD and E. J. KRAMER, *J. Polym. Sci., Polym. Phys. Edn* **20** (1982) 1129.

Received 12 March
and accepted 20 March 1990